Adam CZABAN[*]

CFD ANALYSIS OF THE HYDRODYNAMIC LUBRICATION OF A MISALIGNED, SLIDE CONICAL BEARING

ANALIZA CFD HYDRODYNAMICZNEGO SMAROWANIA STOŻKOWEGO ŁOŻYSKA ŚLIZGOWEGO O NIERÓWNOLEGŁYCH OSIACH CZOPA I PANEWKI

Key words:

hydrodynamic lubrication, sliding bearing, conical, misaligned, CFD, non-Newtonian oil

Słowa kluczowe:

hydrodynamiczne smarowanie, łożysko stożkowe, ślizgowe, nierównoległość osi, CFD, nienewtonowski olej

Abstract

The lateral loads carried by hydrodynamic bearings, and also their uneven distribution, introduce an additional axial misalignment between the shaft and sleeve. The machining and mounting errors also result in improper initial alignment of bearing shaft or sleeve. Furthermore, due to vibrations, misalignment of shaft fluctuates during the operation of the bearing. This has an impact on the operating parameters of the bearing, and, in extreme cases, where the maximum allowable value of the misalignment is exceeded, the

[*] Gdynia Maritime University, ul. Morska 81-87, 81-225 Gdynia, Poland, e-mail: aczaban@am.gdynia.pl.

bearing can be damaged. The aim of this work is to investigate the effect of misalignment on the hydrodynamic pressure distribution in the conical sliding bearing lubrication gap and on the bearing load carrying capacity and friction force values.

This paper shows the result of a CFD simulation of hydrodynamic conical bearings lubrication with the assumption that the bearings are misaligned, i.e. where the rotation axis of bearing shaft is not parallel to the axis of the cone of the bearing sleeve. The commercial CFD software ANSYS Fluent was used in this research. It was assumed that the flow of lubricating oil is laminar, without slipping on bearing surfaces, and that the oil has non-Newtonian properties.

INTRODUCTION

When designing hydrodynamic slide bearings, it is usually assumed in calculations that the rotation axis of the bearing shaft is parallel to the axis of the bearing sleeve. However, during the operation of the bearing, these axes are not parallel. Such misalignment can result from the inaccuracy of the production or the assembly of the bearing; furthermore, the load carried by the bearing increases the difference in the position of the shaft axis in relation to the predetermined nominal axis. This causes significant changes in the height h of the oil gap of bearing and thus the hydrodynamic pressure distribution of lubricating oil in the bearing oil gap, and the lift forces and the frictional forces are also changing. Li *et al.* (2012) in research **[L. 1]** show the results of simulations obtained using the CFD and FSI (*fluid-structure interactions)* methods for the bearing, where the position of the journal axis varies during its operation. He *et al.* (2012) in paper **[L. 2]** present an analysis of the flexible journal misalignment of slide journal bearing based on the "simple step shaft" model. Abass & Kadhim (2013) in work **[L. 3]** made a thermo-hydrodynamic analysis for the misaligned hydrodynamic journal bearing, also taking into account the influence of the roughness of operating bearing surfaces and non-Newtonian effects, which occur during lubrication. Elsharkawy (2007) in research **[L. 4]** studied the effects of oil additives on the hydrodynamic lubrication of slide bearings with the misaligned journal in the conical sleeve. Koprowski (2007) in article **[L. 5]** analysed asymmetrical lubrication gaps of a conical slide bearing, i.e. taking into account the misalignment between axes of bearing shaft and sleeve and including the effect of the difference between opening angles of the cones of bearing shaft and sleeve, but assuming that the lubricating oil has the Newtonian properties. Nowak & Wierzcholski (1984) in work **[L. 6]** was theoretically concerned with the hydrodynamic conical bearing lubricated with Non-Newtonian oil, in which the dependence of stress on shear rate is described by the Ostwald-de Waele

power law model. Paper **[L. 7]** presented a CFD analysis of non-isothermal hydrodynamic lubrication of slide conical bearing assuming that the oil has properties of a Ostwald-de Waele fluid.

This paper shows the results of the simulation of the hydrodynamic lubrication of the slide conical bearing (conical shaft and conical sleeve), taking into account the misalignment between the axes of the bearing shaft and sleeve, i.e. the rotation axis of the bearing shaft is not parallel to the axis of the sleeve. The study was carried out using commercial CFD software Ansys Fluent from the Ansys Workbench platform, which was also used to prepare the geometric model of the bearing, create the mesh, and to analyse the results.

In general, the axes of the bearing shaft and sleeve are not on the same plane. In this study, only a special case is examined, i.e. in which the rotation axis of the bearing shaft is in one plane with the axis of the sleeve and which is also the plane of the so-called *line of centres* (i.e. the line in the plane of the cross-section of the bearing and intersecting the shaft axis and the axis of the sleeve).

MODEL OF OIL FLOW

The geometry of the concerned conical bearing is shown in **Fig. 1**. The misalignment of the shaft axis is defined as the angle ζ between this axis and the nominal axis of shaft (or equivalently, between the axis of the shaft and the axis of the sleeve), indicated in **Fig. 1**.
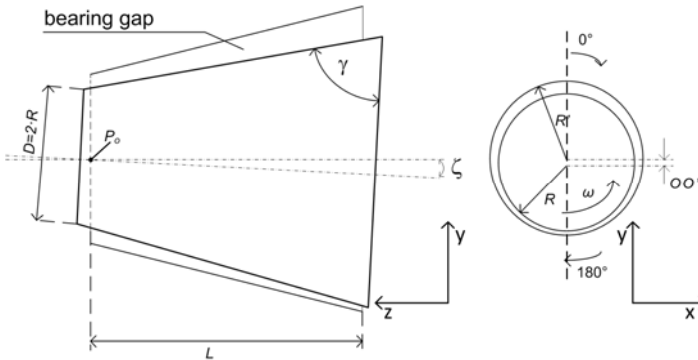

Fig. 1. Geometry of the investigated bearing
Rys. 1. Geometria modelowanego łożyska

It was assumed that the change in the angle ζ value is made by rotating the bearing shaft at a point *Po*. This is the point at which the axis of the bearing shaft pierces the plane of lowest cross-section of the sleeve. In the context of explanation, why the angle ζ was determined as described above, and it is

represented in **Fig. 2** showing a loaded cylindrical shaft supported by two conical bearings.
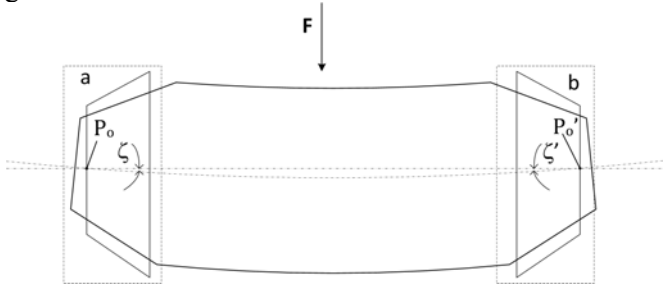

Fig. 2.   Loaded shaft supported by two conical bearings
Rys. 2.   Obciążony wał podparty na dwóch łożyskach stożkowych

The resultant load F causes the deflection of the shaft; therefore, the positions of the conical bearings shafts are changing. In this work, only one conical bearing (show in **Fig. 2** and located in the "a" area) was considered. How the change of in value of angle ζ affects the hydrodynamic pressure distribution and operational parameters of a slide conical bearing is investigated.

The following conditions and assumptions were adopted in the simulations:
1. The bearing length was of $L = 50$ [mm] (measured along the axis of the sleeve).
2. The radius of bearing shaft at its lowest cross section was of $R = 50$ [mm].
3. The opening angle of the shaft cone was equal to the opening angle of the sleeve cone – the angle between the shaft rotation axis and the cone generating line was of 10°, so the indicated in Fig. 1 angle $\gamma = 80°$.
4. The radial clearance, $\varepsilon = R' - R = 0.025$ [mm], is where R' is the radius of the sleeve at its lowest cross section.
5. The bearing operates in a steady state, i.e. when the value of rotational speed is constant, there are no vibrations, and the flow of oil is laminar and incompressible.
6. The flow of lubricating oil was non-isothermal (the parameters of the lubricating oil: density 850 [kg/m^3], specific heat 1006 [J/(kg·K)], heat conduction coefficient 0.025 [W/(m·K)]).
7. The temperature of the shaft surface and also the supplying oil was 90°C.
8. The stationary steel sleeve conducts heat from bearing gap to the surroundings (the parameters of the sleeve material: density $\rho = 8030$ [kg/m^3], specific heat $c_p = 503$ [J/(kg·K)], heat conduction coefficient $\kappa = 16.27$ [W/(m·K)], sleeve thickness $\delta = 1$ [mm].
9. The rotational speed of the shaft is $\omega = 1500$ [rpm].
10. There was no slip of oil at bearing surfaces.

11. The bearing surfaces were smooth, rigid, and without deformations.
12. The pressure on the side surfaces of bearing gap was equal to the ambient pressure.
13. The Gümbel boundary condition **[L. 8]** was imposed.
14. The calculations were done for the following relative eccentricities: λ = 0.4, 0.5, and 0.6,
    where

$$\lambda = \frac{OO'}{\varepsilon}, \tag{1}$$

and OO' [mm] is the absolute value of eccentricity (the nominal distance between the axis of shaft and axis of sleeve).

15. The Ostwald-de Waele **[L. 6]** model was imposed, which describes the dependence of the stress τ [Pa] of oil, on shear rate θ [s^{-1}]:

$$\tau = K \cdot \theta^n, \tag{2}$$

where K = 0.01242 [Pa·s^n] is the flow consistency index and n = 0.9792 [-] is the flow behaviour (power-law) index. The coefficients for that model were determined with the least squares approximation method (with the Statsoft Statistica software) and fitting the curve described by this model to the experimental data, as in paper **[L. 9]**. Similarly to work **[L. 10]**, it was assumed that the lubricating oil has the same viscosity properties as Shell Helix Ultra AV-L at a temperature of 90°C, which was studied in paper **[L. 9]**. In general, the effects of shear rate and temperature on the viscosity of the lubricating oil where included according to the following formula:

$$\eta(\dot{\gamma}, T) = \eta_1(\dot{\gamma}) \cdot H(T), \tag{3}$$

where η_1 [Pa·s] viscosity is dependent on shear rate due to the Ostwald-de Waele relationship (2), while

$$H(T) = \exp\left[\alpha_T \cdot \left(\frac{1}{T} - \frac{1}{T_\alpha}\right)\right] \tag{5}$$

is a factor that introduces the effect of the temperature on the viscosity of the oil. The parameter $\alpha_T = E_a/R$ is the ratio of the activation energy E_a = 5096 [J/kmol] to the thermodynamic constant R = 8314 J/(kmol·K) and T_α [K] is a REFERENCES temperature for which $H(T)$ = 1.

The number of nodes of the generated mesh was of $1.3 \cdot 10^5$ and the number of elements were of $0.9 \ 10^5$.
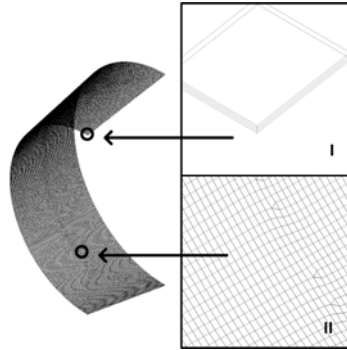
Fig. 3.   An example of the generated mesh for the area of lubrication gap
Rys. 3.   Przykład wygenerowanej siatki w obszarze szczeliny smarnej

The *Pressure Based Coupled method* (Green-Gauss node based, the second order pressure, the momentum second order upwind, and the energy second order upwind) was used in the calculations with the Ansys Fluent solver for solving the equations of motion and determining the values of the pressure and velocity of lubricating oil.

RESULTS

Figures 4, 5, and **6** show the hydrodynamic pressure distributions (longitudinal sections) in the lubrication gaps of concerned bearings, determined along a line passing through a position at which there was a maximum value of pressure (the angular coordinate has a constant value). The length *l* [mm] is the distance measured from the lowest cross-section of the bearing (front of the bearing) along the axis of the bearing sleeve. The arrow indicates an increase in the angle of misalignment ζ. The pressures are in an absolute scale, assuming that the ambient pressure $p_{amb} = 1.013 \cdot 10^5$ [Pa].
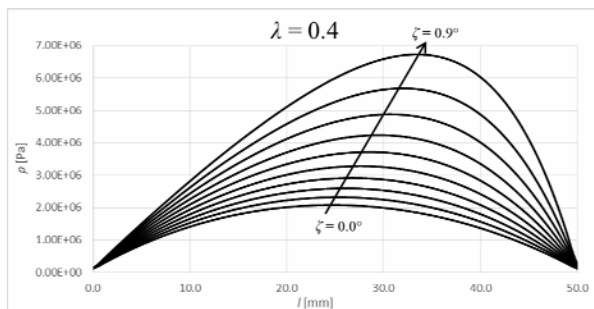

Fig. 4.   The oil pressure in the lubricating gap along a line passing through the position of the maximum pressure for bearing with $\lambda = 0.4$
Rys. 4.   Wartości ciśnienia oleju w szczelinie smarnej wzdłuż linii przechodzącej przez położenie maksymalnego ciśnienia, dla łożyska o $\lambda = 0,4$
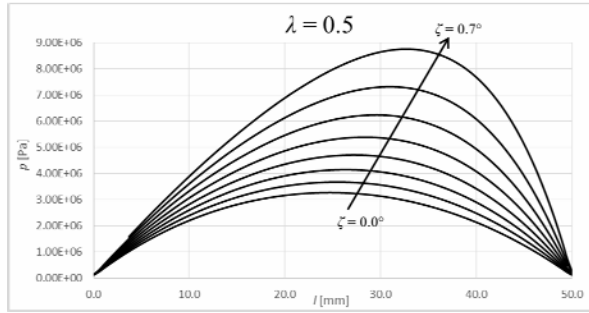
Fig. 5. **The oil pressure in the lubricating gap along a line passing through the position of the maximum pressure for bearing with** $\lambda = 0.5$

Rys. 5. Wartości ciśnienia oleju w szczelinie smarnej wzdłuż linii przechodzącej przez położenie maksymalnego ciśnienia, dla łożyska o $\lambda = 0,5$
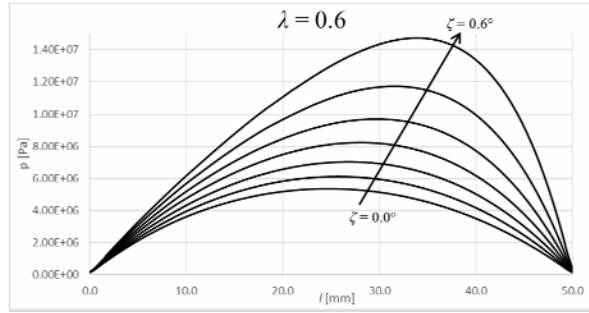

Fig. 6. **The oil pressure in the lubricating gap along a line passing through the position of the maximum pressure for bearing with** $\lambda = 0.6$

Rys. 6. Wartości ciśnienia oleju w szczelinie smarnej wzdłuż linii przechodzącej przez położenie maksymalnego ciśnienia, dla łożyska o $\lambda = 0,6$

Increase of the ζ angle resulted in the generation of larger maximum hydrodynamic pressure p_{max} in the lubrication gap and change in its location, shifting towards the lower gap height. **Fig. 7** shows the change in the position of the maximum value of the pressure in the lubrication gap with respect to angular coordinate and distance from the front of bearing – the increase of the ζ causes the increase of the distance l and increase of the value of angular coordinate φ.
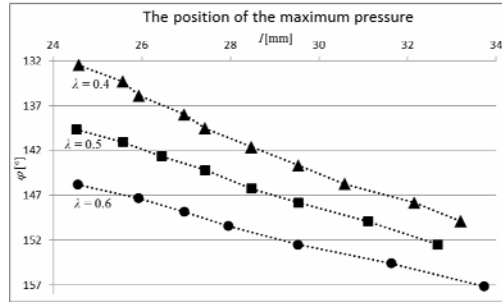
Fig. 7.   The position of maximum pressure for varying angle λ

Rys. 7.   Położenie maksymalnej wartości ciśnienia dla różnych λ

The maximum pressure and the average pressure values for bearings with $\lambda = 0.4$, 0.5, and 0.6 and depending on the value of misalignment are shown in **Figs. 8, 10**, and **12**. The radial C_t (transversal direction) and C_l axial (longitudinal direction) components of load carrying capacity and the friction torques M are shown in **Figs. 9, 11**, and **13**. **Figure 14** shows the maximum values of oil temperature generated in the lubrication gaps of the bearings.
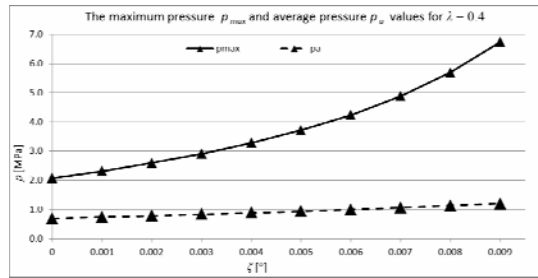

Fig. 8.   The values of maximum and average pressure for varying ζ ($\lambda = 0.4$)

Rys. 8.   Wartości maksymalnego i średniego ciśnienia dla różnych ζ ($\lambda = 0,4$)
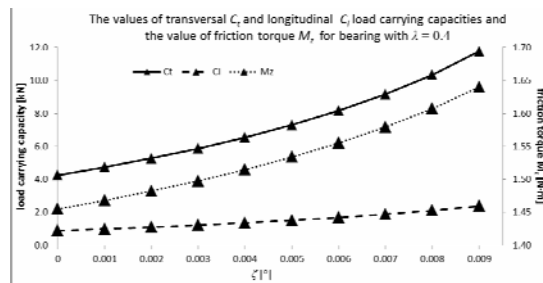

Fig. 9.   The values of axial and radial components of load carrying capacity and value of friction torque for varying ζ, for bearing with $\lambda = 0.4$

Rys. 9.   Wartości składowej osiowej i promieniowej siły nośnej oraz wartość momentu tarcia dla różnych ζ, dla łożyska o $\lambda = 0,4$
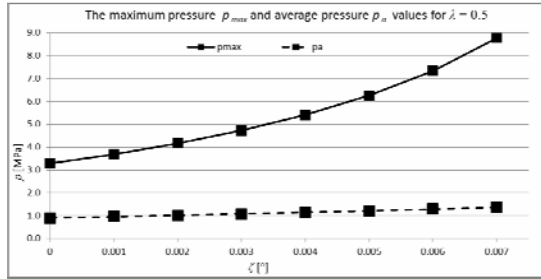
Fig. 10.   The values of maximum and average pressure for varying ζ ($\lambda = 0.5$)

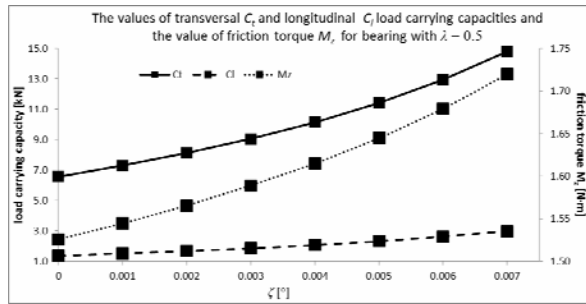Rys. 10.   Wartości maksymalnego i średniego ciśnienia dla różnych ζ ($\lambda = 0,5$)

Fig. 11.   The values of axial and radial components of load carrying capacity and value of friction torque for varying ζ, for bearing with $\lambda = 0.5$

Rys. 11.   Wartości składowej osiowej i promieniowej siły nośnej oraz wartość momentu tarcia dla różnych ζ, dla łożyska o $\lambda = 0,5$
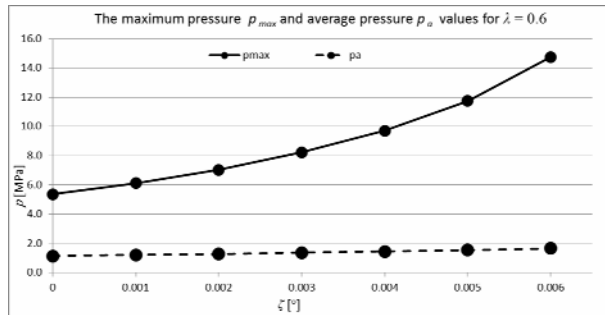

Fig. 12.   The values of maximum and average pressure for varying ζ ($\lambda = 0.6$)

Rys. 12.   Wartości maksymalnego i średniego ciśnienia dla różnych ζ ($\lambda = 0,6$)
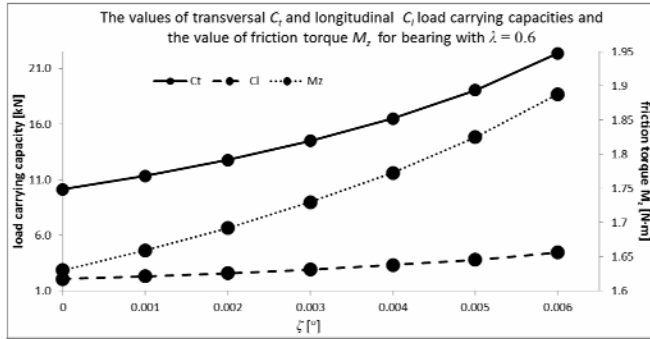
Fig. 13.   The values of axial and radial components of load carrying capacity and value of friction torque for varying ζ, for bearing with $\lambda = 0.6$

Rys. 13. Wartości składowej osiowej i promieniowej siły nośnej oraz wartość momentu tarcia dla różnych ζ, dla łożyska o $\lambda = 0{,}6$
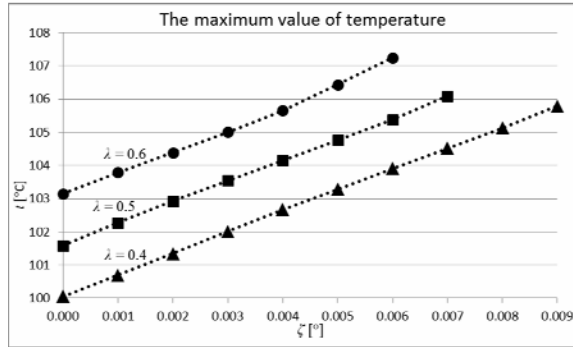

Fig. 14.   The maximum value of oil temperature generated in the lubrication gap

Rys. 14. Maksymalna wartość temperatury oleju w szczelinie smarnej

The maximum value of the angle ζ, for which the simulations were carried out was dependent on the value of relative eccentricity λ. When increasing the value of ζ, the minimum height $h_0 = \min(h)$ of the lubrication gap becomes lower. For greater λ, the contact of surfaces of the shaft and sleeve occurs at the lower misalignments, i.e. angles $\zeta = \zeta_{max}$. The results, however, concern the ζ value in the range from 0.000° to about 80% of ζ_{max} angle at which it comes into the contact of the surfaces of shaft and sleeve, because, for greater values of the ζ, some problems with generating the mesh for the decreasing height of the lubrication gap occurred (this will be investigated in later work).

DISCUSSION AND CONCLUSIONS

This study carried out a simplified analysis of the impact of misalignment between the axes of the shaft and sleeve on the operating parameters of the

hydrodynamic conical bearing. The simulations were made using CFD software. I was assumed that the total volume of half of lubrication gap was filled with oil, for which the classical boundary conditions were imposed, excluding the solid–liquid interaction (without FSI) and considering the misalignment between axes of bearing shaft and sleeve only in one plane. The results show how significantly the operating parameters of the simulated bearing are changed in relation to the planned values, if the misalignment between the axis of the shaft and the axis of the sleeve is taken into account in the calculations. For the examined cases the following can be concluded:

1. For a bearing with $\lambda = 0.4$, when there is an increase of the designated values when $\zeta = 0.009°$, in relation to results when $\zeta = 0.000°$:
$\Delta p_{max} = 224$ %, $\Delta p_a = 73$ %, $\Delta C_l = 170$ %, $\Delta C_t = 177$ %, $\Delta M_z = 12.7$ %,

2. Correspondingly, for $\lambda = 0.5$ and $\zeta = 0.007°$, in relation to $\zeta = 0.000°$:
$\Delta p_{max} = 167$ %, $\Delta p_a = 52$ %, $\Delta C_l = 120$ %, $\Delta C_t = 126$ %, $\Delta M_z = 3.9$ %, and

3. Uniformly, for $\lambda = 0.6$ and $\zeta = 0.006°$, comparing to $\zeta = 0.000°$:
$\Delta p_{max} = 175$ %, $\Delta p_a = 46$ %, $\Delta C_l = 115$ %, $\Delta C_t = 121$ %, $\Delta M_z = 4.2$ %.

It should be noted that increasing the value of angle ζ results in a greater relative increase in the value of C_t component than in the value of C_l component of load carrying capacity, and, consequently, the resultant vector of load carrying capacity generated by the slide conical bearing changes its direction.

The following conclusions were drawn from the studies:

- The simulations demonstrated that the misalignment between the axis of shaft and the axis of sleeve has a significant impact on the hydrodynamic lubrication and operating parameters of the slide conical bearing; therefore, it should be taken into account in calculations.
- Among the benefits of using hydrodynamic slide bearings, the additional advantage of conical bearings is that they can be used in the case where it is necessary to simultaneously carry longitudinal and transverse loads. Unfortunately, this involves a more complicated geometry than in the case of journal (cylindrical) bearing, and it causes difficulties when modelling its operation.
- Commercial CFD software is an excellent tool for solving the hydrodynamic theory of lubrication problems. however, when using such software, which is created for the overall group of issues related to the flows, while simulating operation of slide bearings, one can easily make a lot of modelling mistakes, due to the fact that the height of the layer of lubricating oil of the slide bearing is several orders of magnitude lower than other dimensions of the bearing, which creates a lot of problems of a numerical nature. On the other hand, it allows one to achieve results and values that vary slightly from actually measured values in bearings.

● In the used method, the geometry of the lubrication gap is defined in advance and, for that predefined gap, the hydrodynamic pressure distribution and resultant forces are determined, when in a real case, the gap is formed for a given load, which is a classic approach in the hydrodynamic theory of lubrication of slide bearings – a perspective is a combination of the mechanical and CFD modelling (FSI), which, as write Li *et al.* in paper **[L. 1]**, causes further difficulties and the need to generate a dynamic mesh.

REFERENCES

1. Li Q., Liu S., Pan X., Zheng S., A new method for studying the 3D transient flow of misaligned journal bearings in flexible rotor-bearing systems, Journal of Zhejiang University-SCIENCE A (Applied Physics & Engineering), 13(4), 2012, pp. 293–310.
2. He Z., Zhang J., Xie W., Li Z., Zhang G., Misalignment analysis of journal bearing influenced by asymmetric deflection, based on a simple stepped shaft model, Journal of Zhejiang University-SCIENCE A (Applied Physics & Engineering), 13(9), 2012, pp. 647–664.
3. Abass B.A., Kadhim M.M., Thermo-hydrodynamic Analysis of Misaligned Journal Bearing Considering Surface Roughness and Non-Newtonian Effects, Journal of Engineering, Vol. 19, 2013, No. 5, pp. 637–653.
4. Elsharkawy A.A., Lubricant additives effects on the hydrodynamic lubrication of misaligned conical–cylindrical bearings, Lubrication Science, 19, 2007, pp. 213–229.
5. Koprowski M., Analiza przepływu czynnika smarującego w niesymetrycznej szczelinie smarnej stożkowego łożyska ślizgowego, Polish Maritime Researsch, Vol.14, 2007, No.4 (54), pp. 59–63.
6. Nowak Z., Wierzcholski K., Flow of a Non-Newtonian Power Law Lubricant trough the Conical Bearing gap, Acta Mechanica 50, pp. 221–230, 1984.
7. Czaban A., CFD Analysis of Non-Newtonian and Non-Isothermal Lubrication of Hydrodynamic Conical Bearing, Journal of KONES. Powertrain and Transport., Vol. 21, 2014, No. 4, pp. 49–56.
8. Miszczak A., Analiza hydrodynamicznego smarowania ferrocieczą poprzecznych łożysk ślizgowych, Fundacja Rozwoju Akademii Morskiej, Gdynia, 2006.
9. Czaban A., The Influence of Temperature and Shear Rate on the Viscosity of Selected Motor Oils, Solid State Phenomena, 2013, Vol. 199, pp. 188–193.
10. Czaban A., Cfd Analysis of Non-Newtonian and Non-Isothermal Lubrication of Hydrodynamic Conical Bearing, Journal of KONES, VOL. 21, 2014, No. 4, pp. 49–56.

Streszczenie

Nierównomierny rozkład sił obciążających łożysko ślizgowe, a co za tym idzie – deformacja wału powodują powstawanie nierównoległości pomiędzy osią czopa a osią panewki łożyska. Dodatkowo błędy procesu obróbki lub

montażu elementów łożyska mogą wywołać wstępną nierównoległość pomiędzy osią czopa i osią panewki. Położenie osi czopa nie jest stałe podczas pracy łożyska i zmienia się np. w związku z jego drganiami. Celem tej pracy jest zbadanie wpływu nierównoległości osi obrotu czopa w stosunku do osi panewki na rozkład ciśnienia hydrodynamicznego, wartości sił nośnych i na wartość momentu tarcia w stożkowym łożysku ślizgowym.

W niniejszej pracy zaprezentowano wyniki symulacji CFD dla stożkowego łożyska ślizgowego przy założeniu, że przepływ oleju w szczelinie smarnej jest laminarny. Założono, że olej jest płynem o właściwościach nienewtonowskich, a zależność naprężeń od szybkości ścinania jest opisana relacją Ostwalda de Waele. Symulacje przeprowadzono dzięki wykorzystaniu komercyjnego oprogramowania CFD Ansys Fluent.